NASA Technical Memorandum 102725

LASER TRANSIT ANEMOMETER MEASUREMENTS OF A JANNAF NOZZLE BASE VELOCITY FLOW FIELD

WILLIAM W. HUNTER, JR., C. E RUSS, JR., AND J. I. CLEMMONS, JR.

AUGUST 1990

(NASA-TM-102725) LASER TRANSIT ANEMOMETER MEASUREMENTS OF A JANNAF NOZZLE BASE VELOCITY FLOW FIELD (NASA) 26 p CSCL 14B

N91-12063

Unclas
G3/35 0311546

NASA
National Aeronautics and Space Administration

Langley Research Center
Hampton, Virginia 23665-5225

INTRODUCTION

This report describes measurement results obtained using a laser transit anemometer (LTA) instrument to obtain nonintrusive measurements of the velocity flow field of a nozzle jet exhausting into a supersonic flow (M_∞ = 1.4) in the Air Force Arnold Engineering Development Center (AEDC) 1T Wind Tunnel. This test was the second in a series of three planned tests--one per year--to be conducted at AEDC using the NASA Langley Research Center (LaRC) LTA instrument. These cooperative experiments are part of a formal interlaboratory Memorandum of Agreement between the NASA LaRC, the NASA Lewis Research Center (LeRC) and the AEDC to investigate the LTA technique and to develop an advanced LTA instrument for aerodynamic research facility nonintrusive measurements.

The overall goal of this second series of tests was to explore the performance of the LTA instrument in a series of complex flows generated by the nozzle jet exhausting into a supersonic flow field. The results of the LTA measurements are to be compared by the AEDC personnel with flow visualization surveys previously conducted and laser Doppler velocimeter (LDV) measurements to be performed. The results of the comparisons will be used to evaluate performance capabilities and limitations of the LTA instrument.

SYMBOLS

B	background value
i	integer
M_{je}	nozzle jet Mach number
M_∞	tunnel free stream Mach number
n_i	number of events occurring with transit time t_i
P	peakness
R	range of valid transit events

S	skewness
SS	spot separation
$\bar{V}$	local mean velocity
Y(J)	correlogram store number, integer
X,Y,Z	Cartesian coordinates
σ^2	variance
τ_i	transit time of the ith event
$\bar{\tau}$	mean transit time
$\Delta\tau$	counting time interval

APPARATUS

Laser Transit Anemometer

The LTA system utilized in this experiment was a Spectron Development Laboratories, Inc., Model 104. See reference 1 for detailed description of the basic electro-optics and signal processing concepts. The LTA measures the transit time of particles that cross two focused laser beams. The optical package sketched in figure 1 forms "two spots" in space and detects light scattered from particles upon passage through each spot. Detected signals are correlated in time with a correlation device, the correlex, with a maximum time resolution of 10 nanoseconds. LTA system control, data acquisition, and data processing is performed by a microprocessor based computer system.

The optics package is designed so that the plane formed by the optical axes of the two beams may be rotated about an axis that is midway between the two beams. This capability permits the determination of the flow angle using a "best angle" search. The procedure is to make velocity magnitude measurements at several spot rotation angles at fixed preselected incremental angles. A plot is then made of the "two spot" angular position against contrast. Contrast is defined as:

$$\text{contrast} = \frac{1/3(Y(J+1) + Y(J) + Y(J-1)) - B}{B}$$

where B is a background value, Y(J) is the peak correlogram value and Y(J+1) and Y(J-1) are correlogram values on each side of the peak, Y(J). A least squares fit of a parabolic equation through the maximum three adjacent contrast angle positions is performed and the abscissa of the parabolic vertex is taken to be the mean flow angle or best angle. Finally, the system is positioned at this angle and a velocity magnitude measurement is performed.

The LTA system has a specified angular resolution capability limited to 0.1 degrees, which is limited by its electromechanical rotation mechanism. For the current experiment the transceiver lens focal length was 881 millimeters, the spot separation was 1.249 millimeters and the diameter of each spot was approximately 30 micrometers at the $1/e^2$ point.

EXPERIMENTAL PROCEDURES

LTA System Alignment

Precise alignment of a laser/optical system such as the LTA system with respect to a wind tunnel model is necessary to achieve an accurate flow field picture near model surfaces. The LTA laser/optics head was positioned on a three-dimensional scan rig with positioning control and readout precision of ± 25.4 micrometers (± 0.001 inch). The face of the LTA laser/optics head was located approximately 925 millimeters (36.5 inches) from the tunnel center line.The laser beams were projected through two tunnel windows; one located in the plenum chamber side wall, 25.4 millimeters (1.0 inch) thick and the second located in the test section side wall, 38.1 millimeters (1.5 inches) thick. Both windows were made of optical grade glass.

The scan platform upon which the LTA head was placed was leveled and aligned parallel with the tunnel side wall. This platform provided a horizontal surface for the optics head which was checked by observing the relative alignment of the two spots when rotated to a position normal to the platform surface. This check was performed by noting the relative positions of the two spots on a plumb line. Both spots fell on the line which indicated the relative positions were within ±0.1 degree to true normal. Next, the LTA laser/optics head was aligned so that reflections from the windows fell upon the transmission aperture of the LTA optics. This procedure not only reduced the background scatter into the LTA receiving aperture to an insignificant amount but also provided a rough method of achieving an alignment of the optical axis of the LTA optics normal to the tunnel side walls. The preceding alignment was achieved by using a piece of fine mesh screen which permitted reasonably unobstructed laser beam transmission and also provided a surface upon which to observe the reflected laser light off the window surface.

The next task was to locate the LTA system's two spots with respect to a model reference point. The location procedure was to operate the LTA laser at its nominal power of 225 milliwatts, single line at 488.0 nanometers. The incident power on the model reference points was reduced to a safe observable level by stacking a No. 2 and a No. 3 neutral density filter in front of the LTA objective lens. A 32 power telescope was mounted on the scan platform and the reduced power spots located on the scribe mark were observed. First, the two spots were rotated to the vertical position and the scan platform positioned in the tunnel flow direction to position the spots on the vertical scribe mark. This set the relative scan platform and therefore the LTA optics in the X-direction. Next, the spots were rotated to the horizontal position and aligned with the horizontal scribe mark. This set the relative Z-direction. Finally, the transverse Y-direction was set by translating the scan platform normal to the model side wall and noting the speckle pattern of the scattered light from the two spots. Maximum speckle size occurs when the central waist point of each spot is located at the model surface. These preceding steps established the relative model, LTA sample volume, and scan platform positions.

DATA ANALYSIS

Measurement (Tau) Space

The fundamental measurement of the LTA system is the transit time of a scattering particulate crossing the "two spots." Assuming that the radiation scattering particles faithfully represent the local flow field conditions in which they are embedded, an estimate of the flow field velocity conditions can be made. An ensemble of transit measurements is assembled. A statistical evaluation of the ensemble provides a measurement of the mean and higher order moments of velocity. The ensemble of transit time measurements is displayed in a plot of number events versus transit time, tau, i.e., a correlogram. The correlogram is displayed on-line in real time and is the researcher's visual representation of the measurement process and raw results. The counting time interval of the tau measurements, delta tau, is operator selectable and can range from 10 nanoseconds to 800 milliseconds.

The data reduction software provided with the LTA system calculates the mean velocity by estimating the mean transit time that is,

$$\bar{V} = SS/\bar{\tau} \tag{1}$$

and

$$\bar{\tau} = \Sigma\, n_i\, \tau_i / \Sigma n_i. \tag{2}$$

where $\bar{V}$ is the mean velocity, SS is the spot separation, $\bar{\tau}$ is mean transit time, τ_i is the indicated time of the ith particle and n_i the number of events occurring with elapse time of τ_i.

$$\tau_i = i\Delta\tau \tag{3}$$

In the above equation, $\Delta\tau$ is the counting time interval and i is an integer indicating the number of elapse time intervals.

To further improve the precision of the mean velocity estimate, the LTA system software includes a routine for estimating an average "background" level. The background level, B, contribution is then subtracted uniformly from the data set, i.e.,

$$(n_i - B). \tag{4}$$

Now the estimate of the mean transit time $\bar{\tau}$, is determined by:

$$\bar{\tau} = \Sigma (n_i - B)\, \tau_i / \Sigma\ (n_i - B) \tag{5}$$

The essence of the background estimating procedure is to determine τ_i (peak) with the peak n_i value. Select a range, R, about τ_i (peak) based on the number of counting time intervals, e.g., 256. The range R established the "good" data τ_i range. τ_i values outside this range are assumed to contain events due to background contributions only. The average background level is calculated from this data outside range R. This procedure is reasonable as long as the τ_i distribution is well behaved, i.e., single peaked and narrowly distributed in tau space.

Velocity Space

As noted previously, data analysis is routinely performed in measurement or tau space coordinates. This section puts forth considerations for data analysis in velocity space coordinates, $1/\tau_i$. Beginning with

$$Vi = SS/i\Delta\tau \tag{6}$$

A statistical mean estimate is performed where

$$\bar{V} = \frac{\Sigma n_i V_i}{\Sigma n_i} \tag{7}$$

$$\bar{V} = \frac{\Sigma n_i\ (SS/i\Delta\tau)}{\Sigma n_i} \tag{8}$$

$$\bar{V} = \frac{SS}{\Delta\tau}\ \frac{\Sigma n_i/i}{\Sigma n_i} \tag{9}$$

But, the above expressions are not complete because of the nonlinear relation between Vi and τ_i. To account for this nonlinear relation, a weighting factor is incorporated in the statistical analyses. The weighting factor Wi choice is based on the following notion. Consider the relative change of Vi with τ_i. Using equation (6)

$$\Delta Vi = - \frac{SS}{i^2 \Delta\tau} \Delta i \tag{10}$$

For a unit change in Δi then

$$\Delta Vi = \left| \frac{SS}{i^2 \Delta\tau} \right| \tag{11}$$

The velocity resolution per increment i is inversely proportional to i^2. The smallest transition time, τ_i, has a larger velocity acceptance bandwidth compared with a long transit time base on the same counting time increment, $\Delta\tau$. This means that for a uniform velocity distribution the lower ith channels will have a higher probability of acquiring counts, ni, then higher ith channels. Therefore, the weighting factor, Wi, is taken to be inversely proportional to the velocity bandwidth, ΔVi. Therefore, from equation 7,

$$\bar{V} = \frac{\Sigma W_i n_i V_i}{\Sigma W_i n_i} \tag{12}$$

with the result

$$\bar{V} = \frac{SS}{\Delta\tau} \frac{\Sigma i n_i}{\Sigma i^2 n_i} \tag{13}$$

Measurement precision is improved with background removal. Now the estimate mean velocity V, is determined by:

$$\bar{V} = \frac{S \; \Sigma i(n_i - B)}{\Delta\tau \; \Sigma i^2(n_i - B)} \tag{14}$$

Higher order moments are calculated from the following equations. The variance σ^2, is estimated from:

$$\sigma^2 = \frac{\Sigma \; i^2(n_i - B)(V_i - \bar{V})^2}{\Sigma \; i^2(n_i - B)} \tag{15}$$

The third moment, skewness, S, is calculates using:

$$S = \frac{\Sigma \; i^2(n_i - B)(V_i - \bar{V})^3}{\sigma^3 \; \Sigma \; i^2(n_i - B)} \tag{16}$$

and the peakness, P, is determined by:

$$P = \frac{\Sigma \; i^2(n_i - B)(V_i - \bar{V})^4}{\sigma^4 \; \Sigma \; i^2(n_i - B)} \tag{17}$$

Test Program

The purpose of this test program was to obtain velocity vector flow field measurements about a cylindrical body which contained a nozzle jet exhausting from its base in the downstream direction. The nozzle was installed in AEDC's 1T-Transonic Tunnel. The tunnel was operated at M_∞ = 1.4 and the nozzle was operated at M_{je} = 2.4 with a total pressure of 2.41 x 10^6 n/m^2 (350 psi). The nozzle's cylindrical body was 38.1mm (1.5 inches) in diameter. All coordinates in this report are referenced to the origin located at the nozzle base and centerline. All measurements were made in the X-Z plane, i.e., Y - 0.0mm, which is normal to the LTA optical axis.

Test Results

The flow visualization shadowgraph, figure 2, shows the general characteristics of the flow field. Figure 3 contains a composite of velocity vector measurement results obtained with the LTA system. The base of the vectors indicate the measurement location, the vector length and direction, the measured velocity magnitude, and the local flow field direction. Measurements shown in figure 3 were obtained at the X-positions of -76.2mm, -5.1mm, 1.5mm, and 76.2mm. Details of these results are shown in shown in figures 4 through 14.

Figures 4 and 5 contain the results of two surveys performed at the -76.2mm position. The left hand vector set (a) was obtained for a nozzle total pressure condition of 2.41×10^6 n/m^2 (350 psi) and the right hand vector set (b) for nozzle condition of approximately 3.45×10^5 n/m^2 (50 psi). The effects on the boundary layer velocity distribution are shown. The (b) data set of figures 4 and 5 is the only set taken for a different nozzle condition.

Figures 6 and 7 compare velocity vector results obtained at X-positions of -76.2mm and -5.1mm. The righthand vector set (b) was obtained in a region where a separated flow field condition existed because of the effects of the under-expanded nozzle flow field. A distinct difference in the velocity gradients is noted in the region near the cylinder surface. The gap in the velocity data of set (b) is due to the inability to obtain recognizable correlograms. This may be attributable to several causes: (1) Lack of scattering particles, (2) improper selection of time interval base for the correlograms, (3) system noise, etc., and/or (4) limitation on the present LTA system to measure low velocities because of present discrimination range capability.

Figures 8, 9, and 10 are velocity vector presentations of data obtained at the X-position of 76.2mm. The measurements in these figures cross a mixing region of the flow field formed by the nozzle plume and the tunnel free stream behind a wall reflected shock. Essentially two classes of results were obtained with the LTA which represented a multimode velocity distribution both in magnitude and angle. Figure 9 is the results obtained when the flow field characteristics of the free stream are tracked until they are no longer discernable. Figure 10 is the results obtained when the characteristics of the plume are tracked.

The velocity vector profile of the nozzle base plume at the X-position of 1.5mm is shown in figure 11. Velocity measurements along the nozzle centerline are shown in figures 12, 13, and 14.

The LTA measurements indicate that the nozzle plume shock disc was located between 164.6mm and 165.1mm downstream of the nozzle base. The correlograms were single peaked up to position 164.6mm but a double peaked correlogram was noted at 165.1mm with a resultant decrease in the local mean velocity. Complex correlograms were noted after 165.1mm position and persisted until 203.2mm station.

REFERENCES

1. "Photon Correlation Techniques in Fluid Mechanics," Proceedings from the 4th International Conference, Joint Institute for Aeronautics and Acoustics, Stanford University, Stanford, California, August 24-27, 1980. Edited by: W. T. Mayo and A. E. Smart, pp. I-1 through II-36.

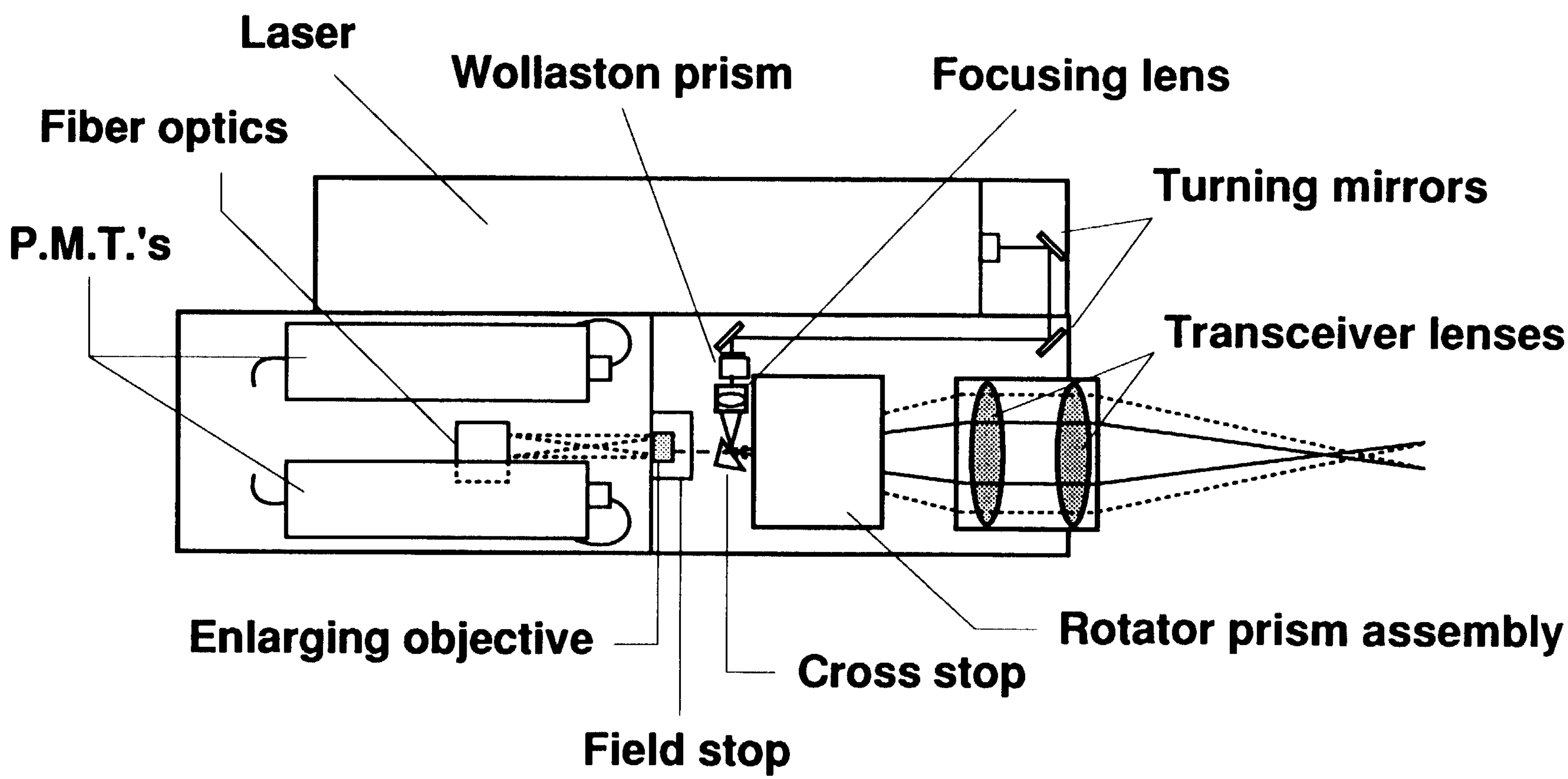

Figure 1. - LTA Laser/Optical Package

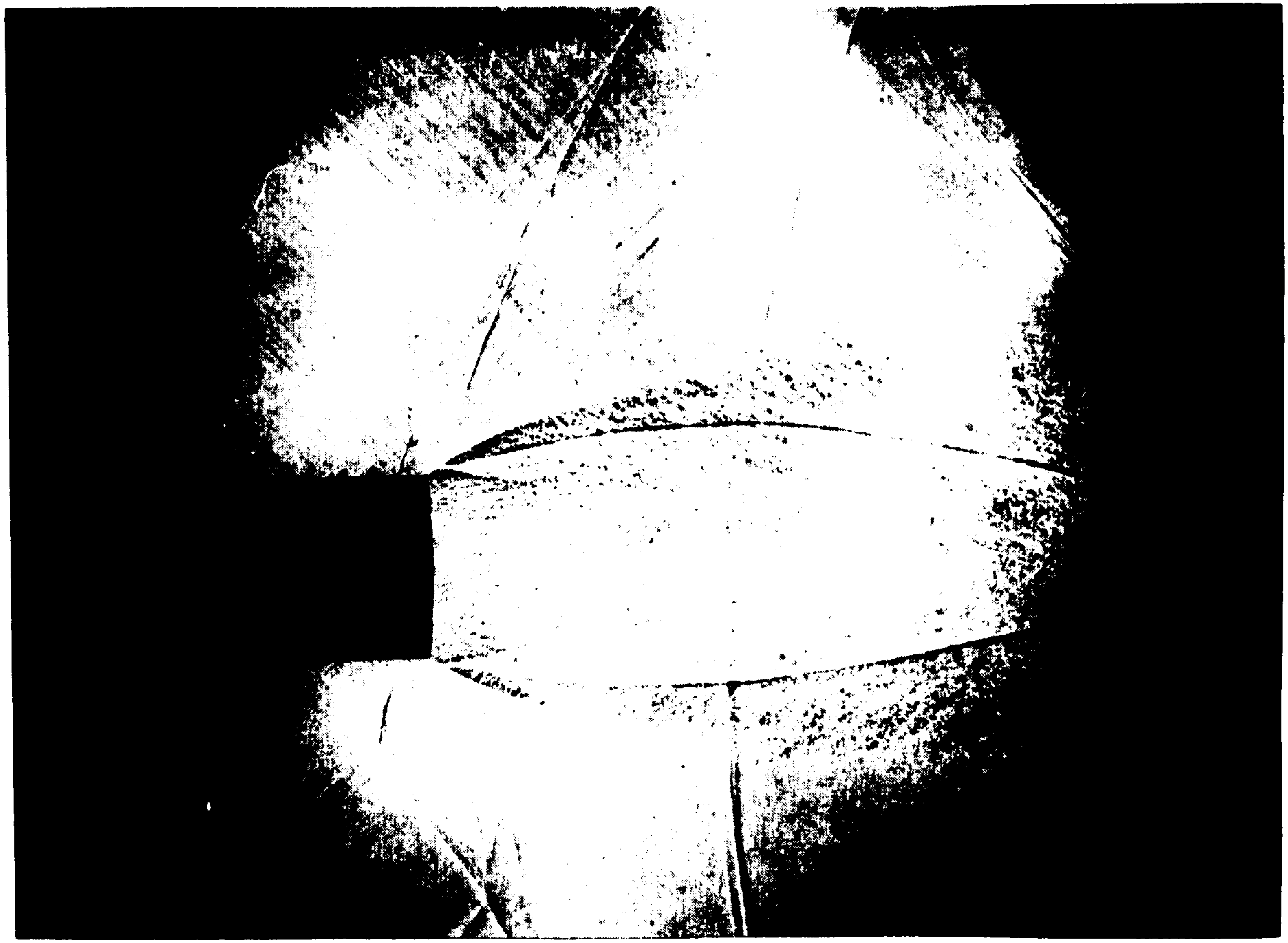

Figure 2. - Shadowgraph of the nozzle jet flow field, $M_{je} = 2.4$, in a $M_\infty = 1.4$ tunnel flow.

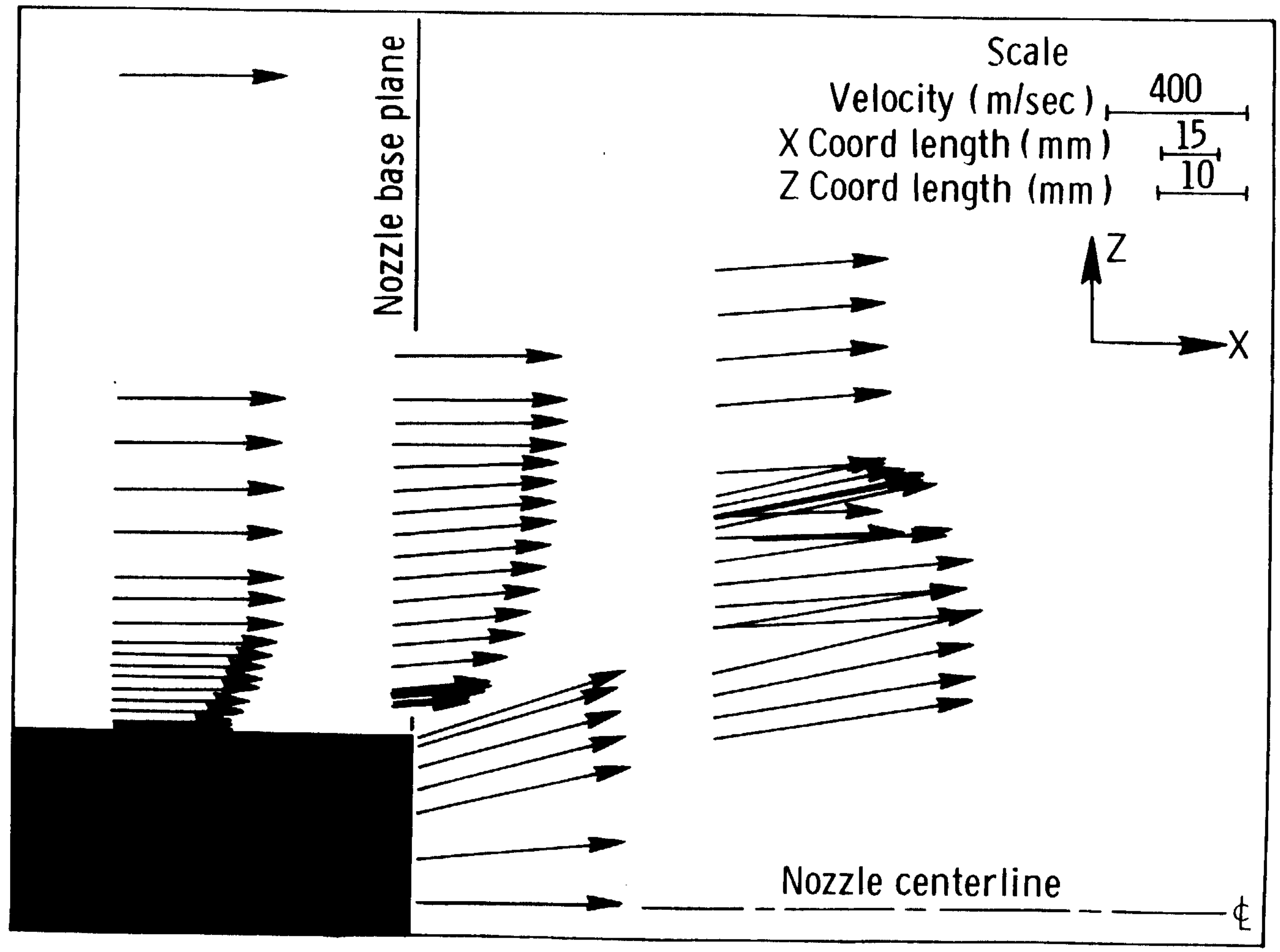

Figure 3. - Composite of velocity vector flow field measurements performed relative to nozzle. Tunnel and nozzle conditions were approximately, $M_\infty = 1.4$ and $M_{je} = 2.4$, respectively.

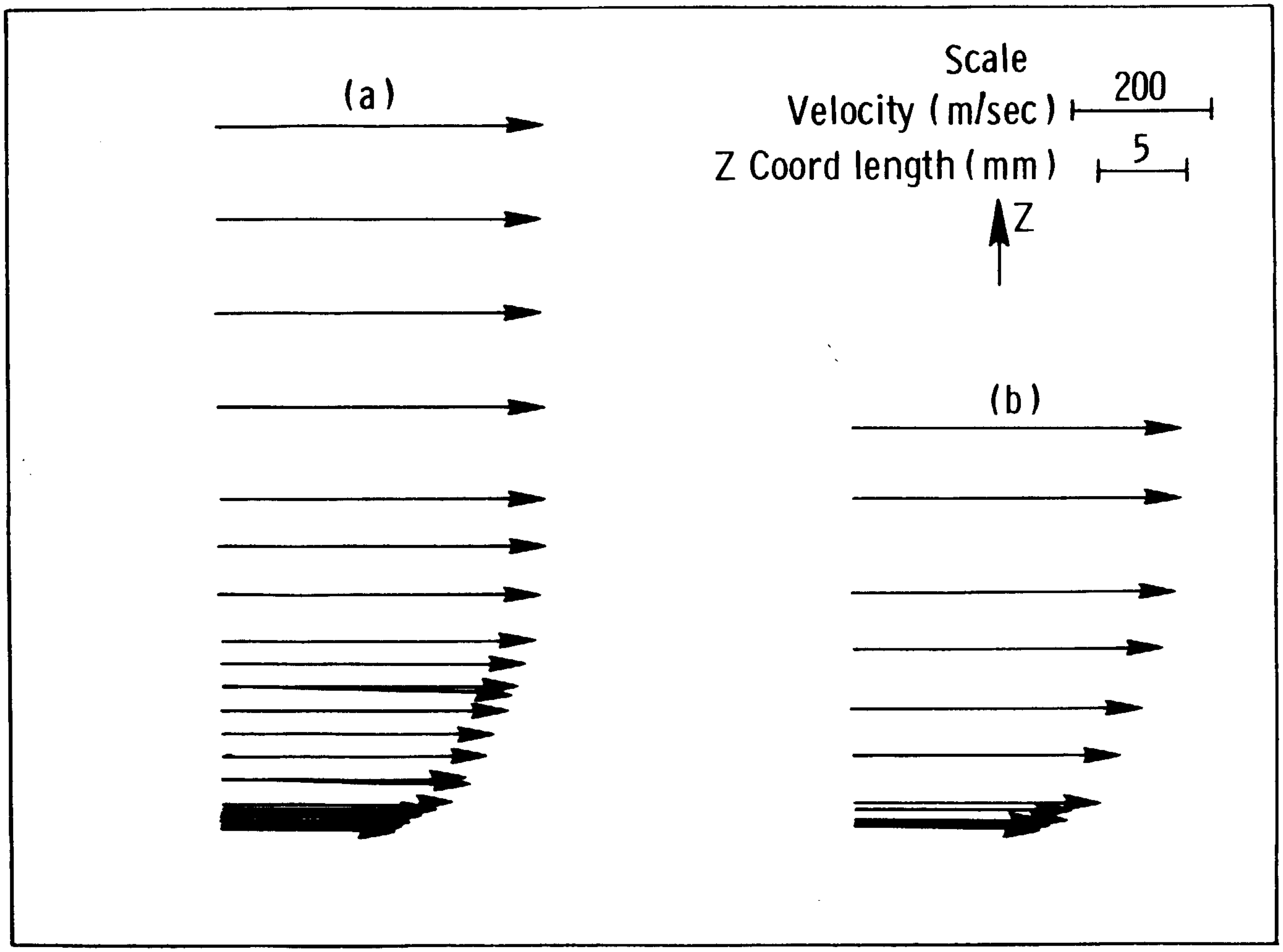

Figure 4. - Comparison of boundary layer velocity vector measurements at X-position coordinate of -76.2 mm with respect to nozzle face plane. Data set (a) measurements for $P_T = 2.41 \times 10^6$ n/m^2 (350 psi) and date set (b) measurements for $P_T = 3.45 \times 10^5$ n/m^2 (50 psi) nozzle conditions. Tunnel condition was $M_\infty = 1.4$. Z-coordinate range is 19.07 to 57.10 mm.

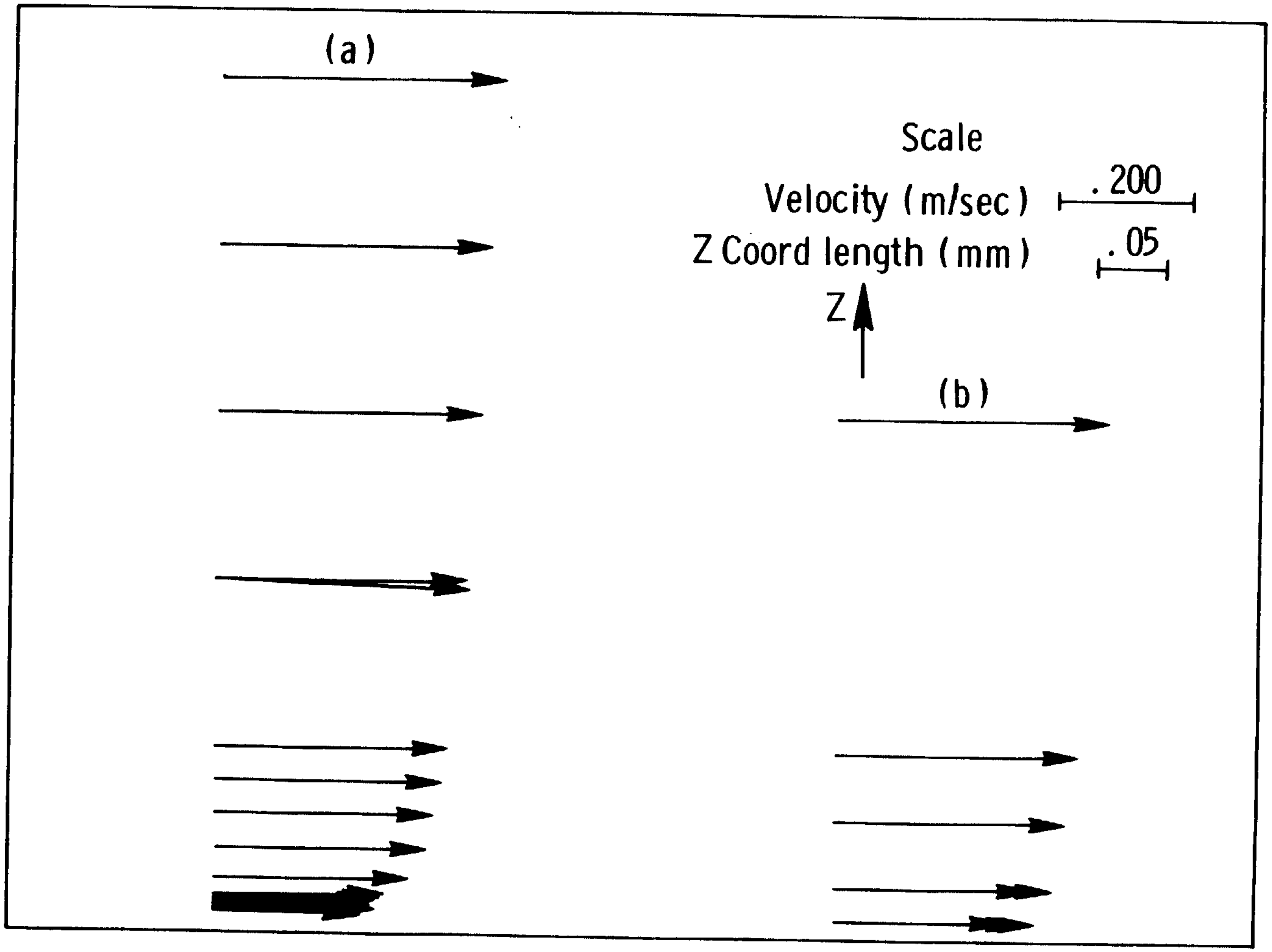

Figure 5. - Comparison of boundary layer velocity measurements at X-position coordinate of -76.2 mm with respect to nozzle face plane. Data set measurements (a) for $P_T = 2.4 \times 10^6$ n/m^2 (350 psi) and (b) for $P_T = 3.45 \times 10^5$ n/m^2 (50 psi) nozzle conditions. Tunnel conditions was $M_\infty = 1.4$. Z-coordinate range is 19.07 to 25.40 mm.

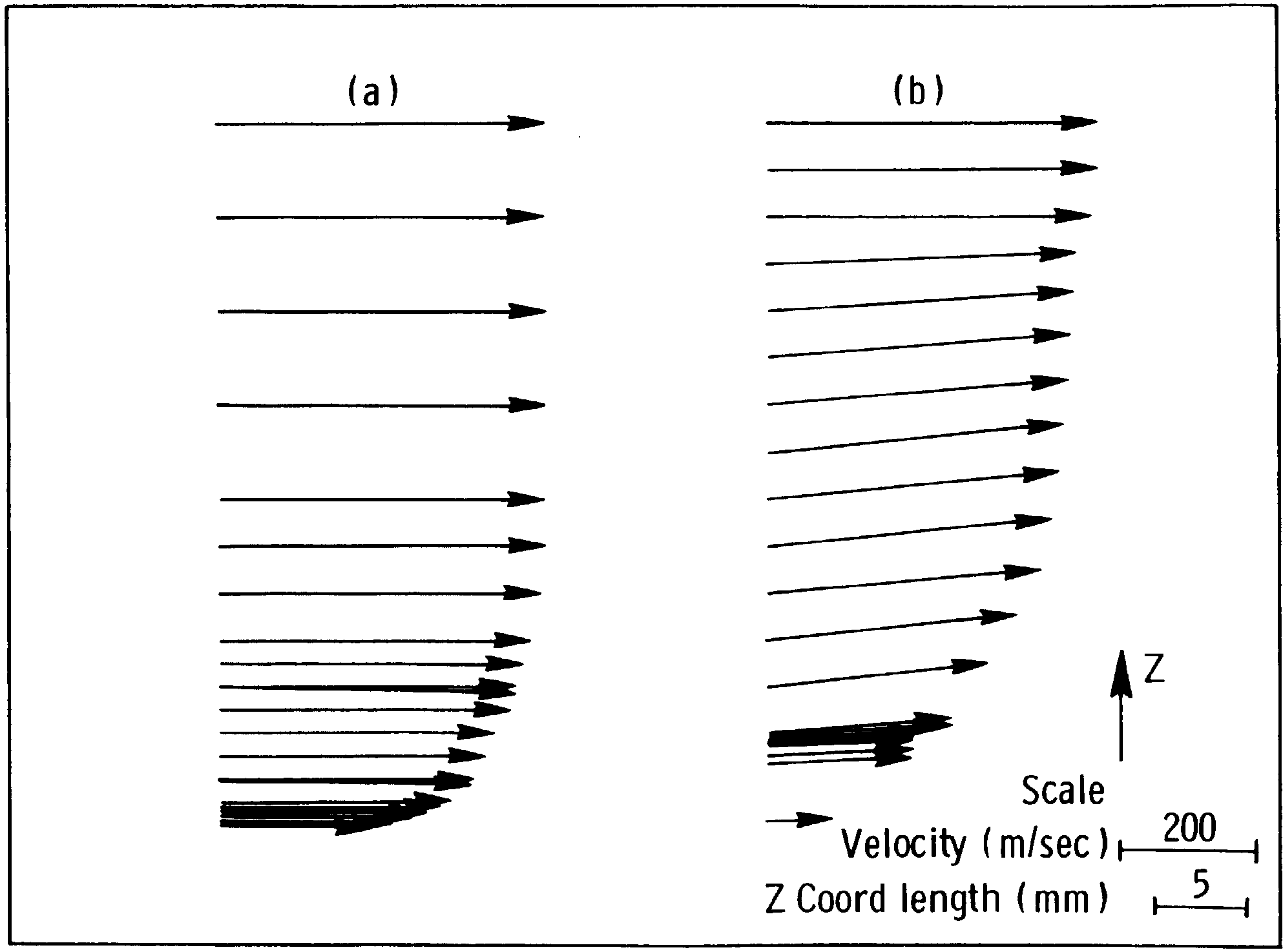

Figure 6. - Comparison of boundary layer velocity vector measurements at X-positions of -76.2 mm, set (a) and -5.1 mm, set (b) with respect to nozzle face plane for same tunnel and nozzle conditions of approximately $M_\infty = 1.4$ and $M_{je} = 2.4$. Z-coordinate range is 19.07 to 57.10 mm.

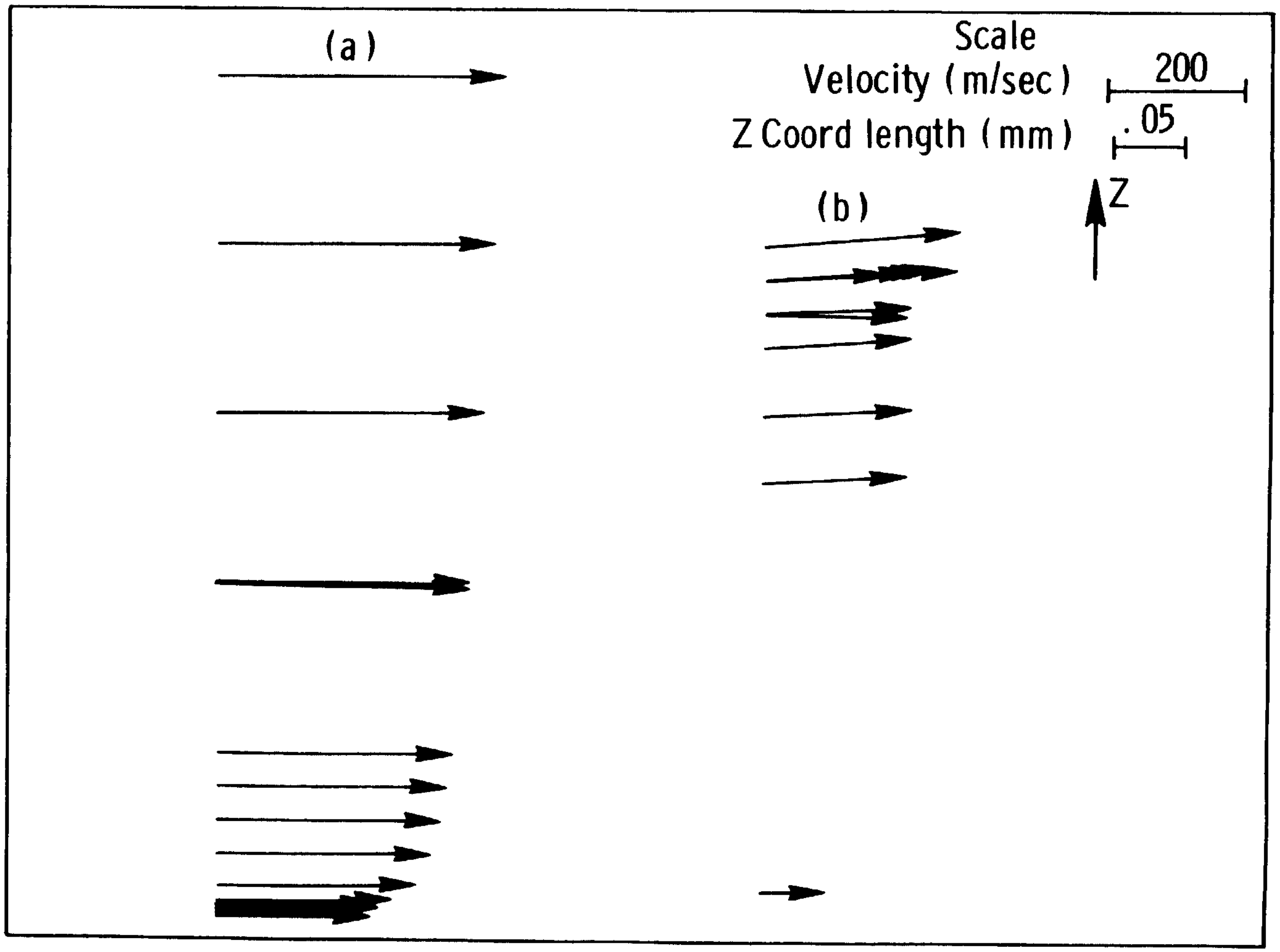

Figure 7. - Comparison of boundary layer velocity vector measurements at X-positions of -76.2 mm, set (a), and -5.1 mm, set (b), with respect to nozzle face plane for similar tunnel and nozzle conditions of M_∞ = 1.4 and M_{je} = 2.4. Z-coordinate range is 19.07 to 25.40 mm.

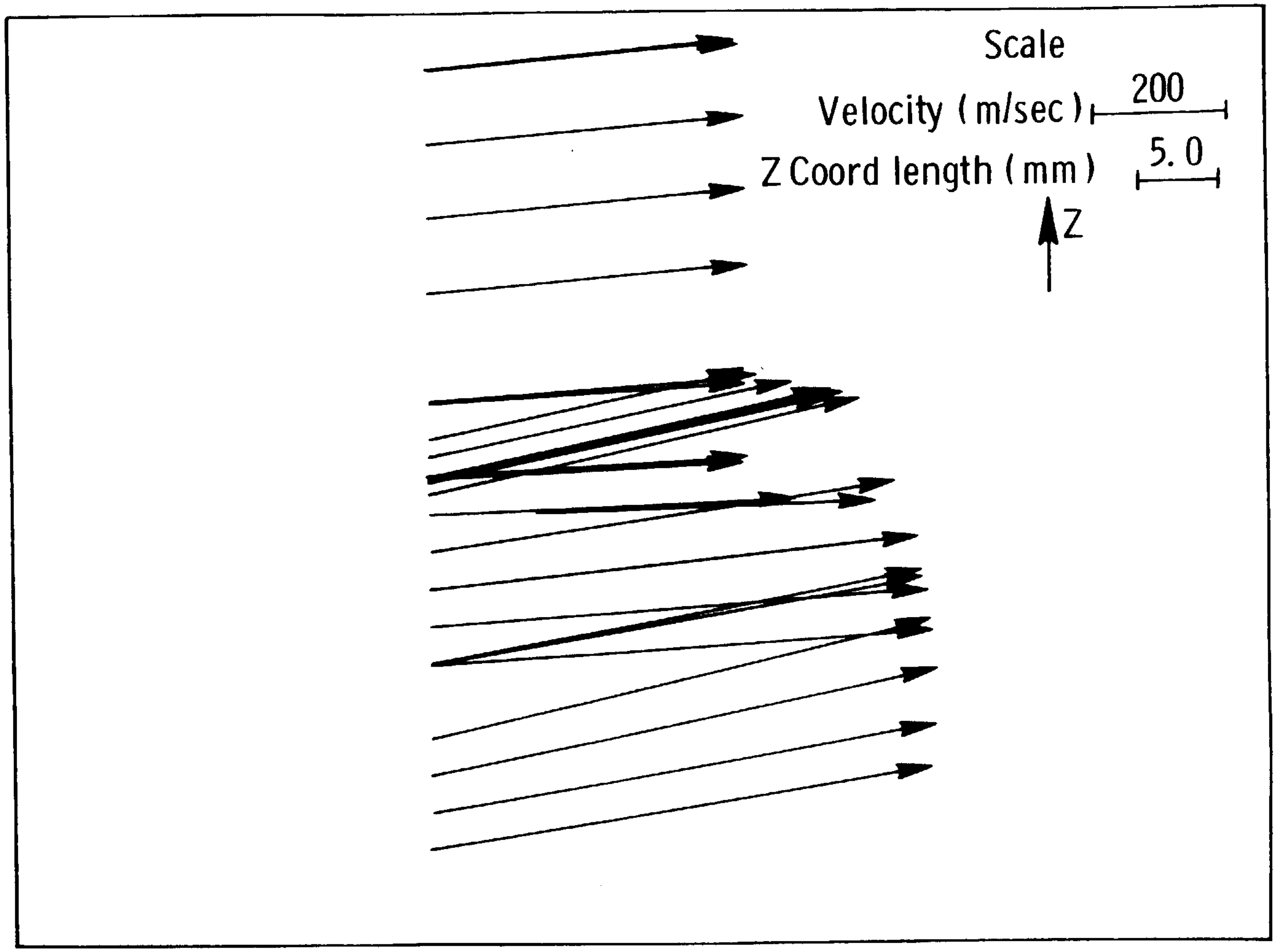

Figure 8. - Velocity vector measurements at X-positions of 76.2 mm with respect to the nozzle face plane for tunnel and nozzle conditions of approximately $m_\infty = 1.4$ and $M_{je} = 2.4$. Z-coordinate range is 19.10 to 72.40 mm.

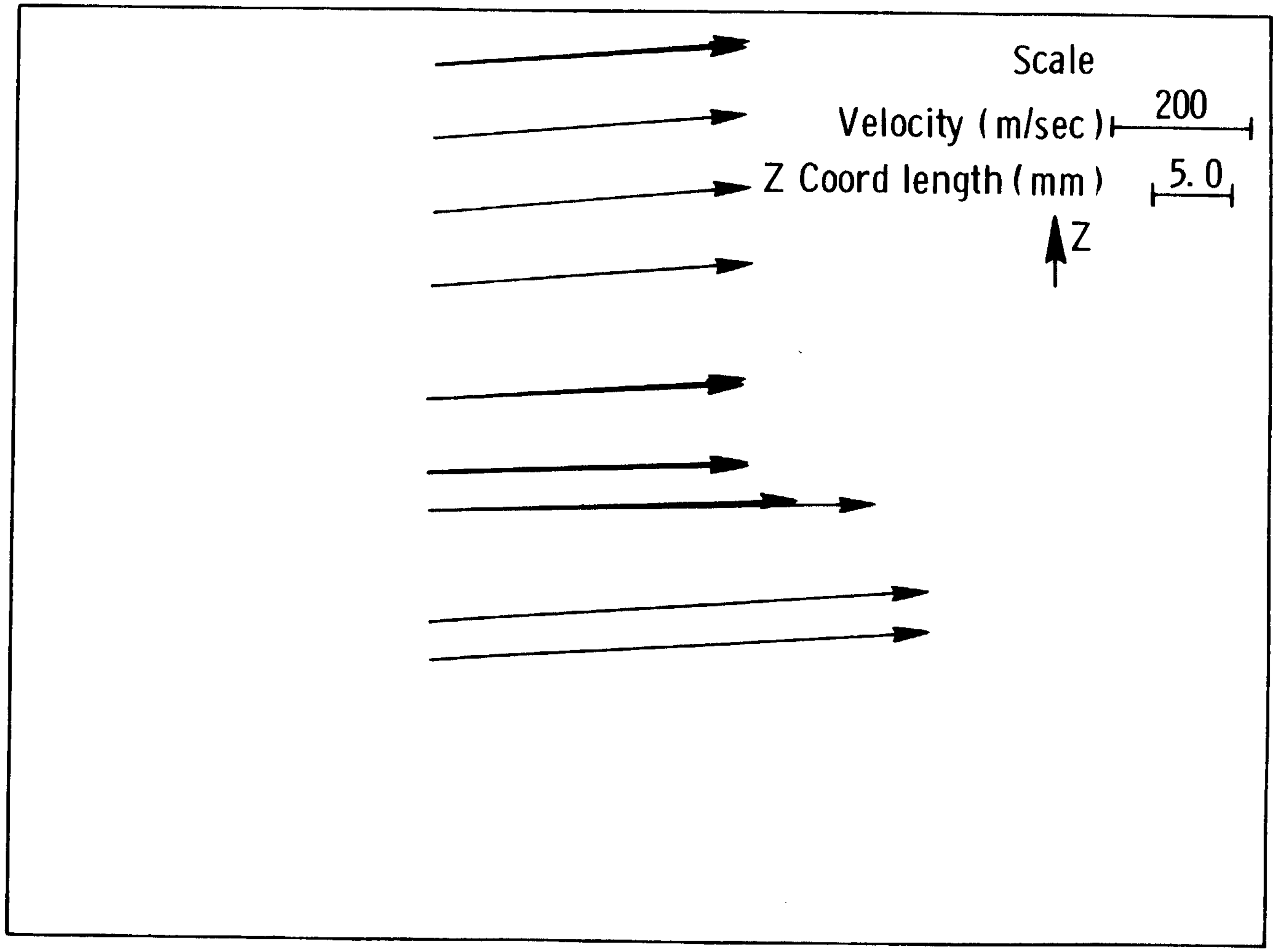

Figure 9. - Velocity vector measurements at X-position of 76.2 mm with respect to the nozzle face plane exhibiting flow field/particle conditions originating outside of the nozzle jet plume. Tunnel and nozzle conditions were approximately $M_\infty = 1.4$ and $M_{je} = 2.4$. Z-coordinate range is 31.80 to 72.40 mm.

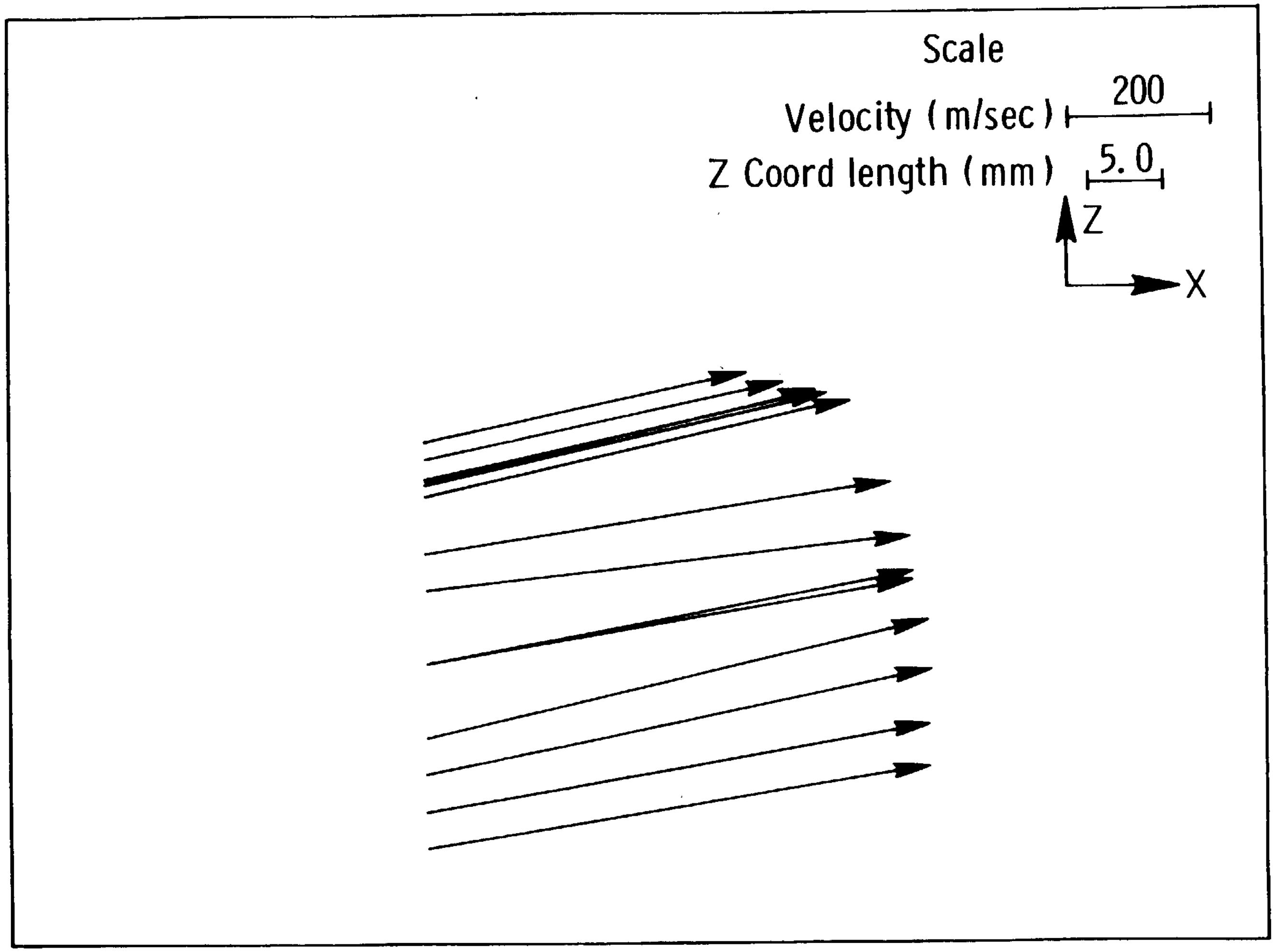

Figure 10. - Velocity vector measurements at X-position of 76.2 mm with respect to the nozzle face plane exhibiting flow field/particle conditions originating inside of nozzle jet plume. Tunnel and nozzle conditions were approximately $M_\infty = 1.4$ and $M_{je} = 2.4$. Z-coordinate range is 19.10 to 47.00 mm.

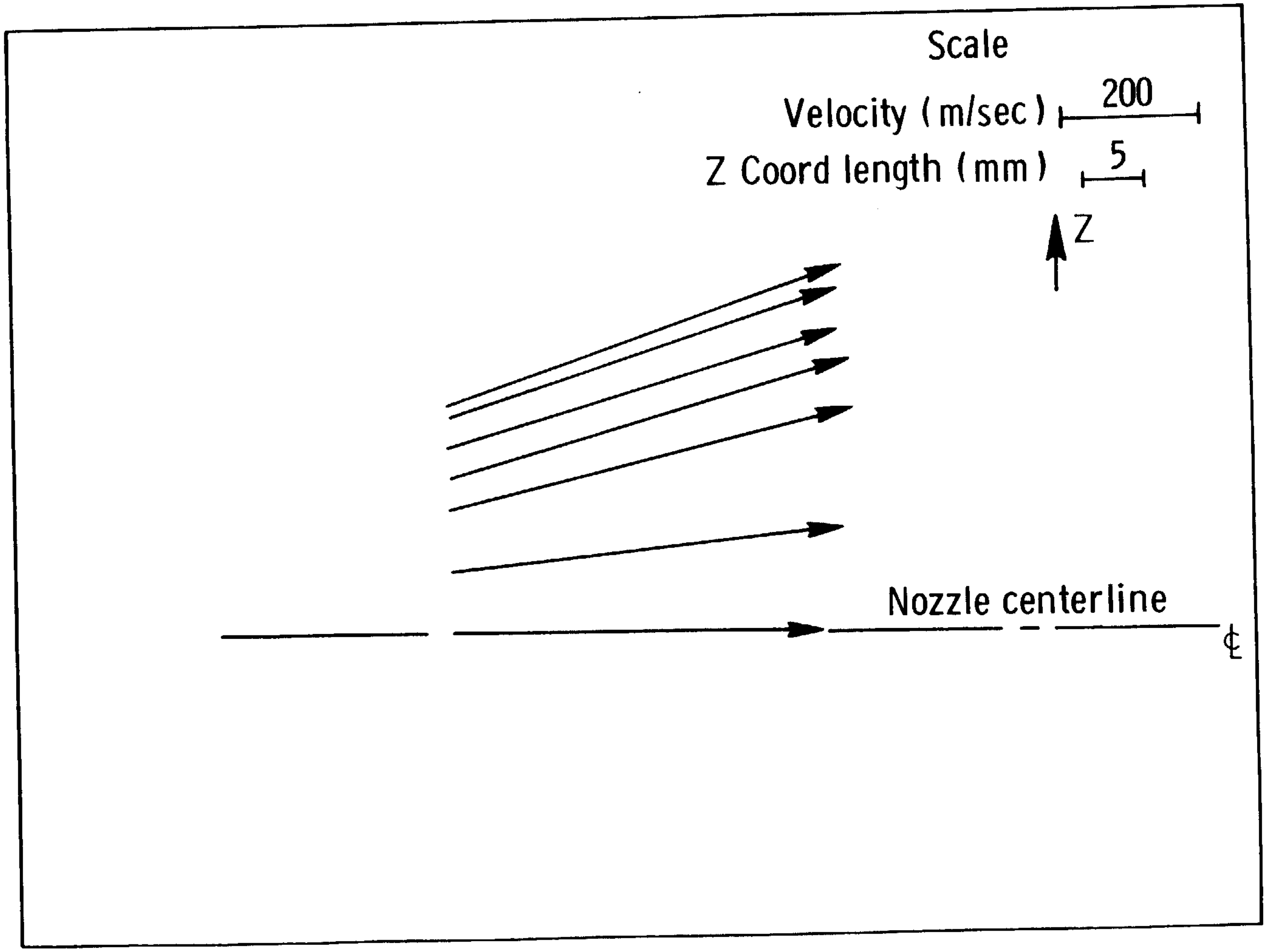

Figure 11. - Velocity vector measurements at X-position of 1.5 mm with respect to the nozzle face plane for tunnel and nozzle conditions of $M_\infty = 1.4$ and $M_{je} = 2.4$. Z-coordinate range is 0.00 to 18.66 mm.

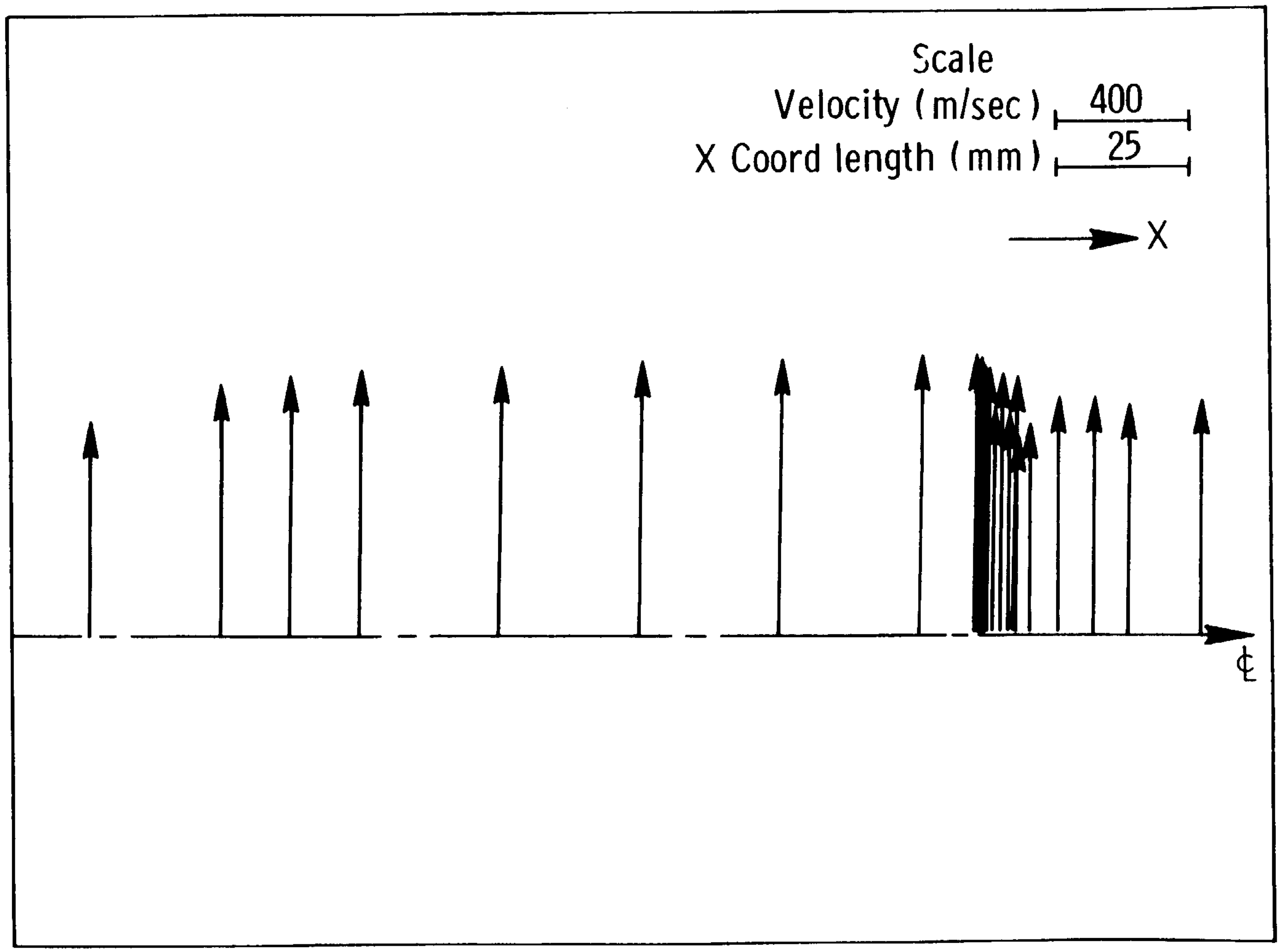

Figure 12. - Velocity vector measurements along nozzle centerline, Z-position 0.00 mm. Velocity vectors rotated 90° ccw for clarity of presentation. X-coordinate range is 1.50 to 203.20 mm.

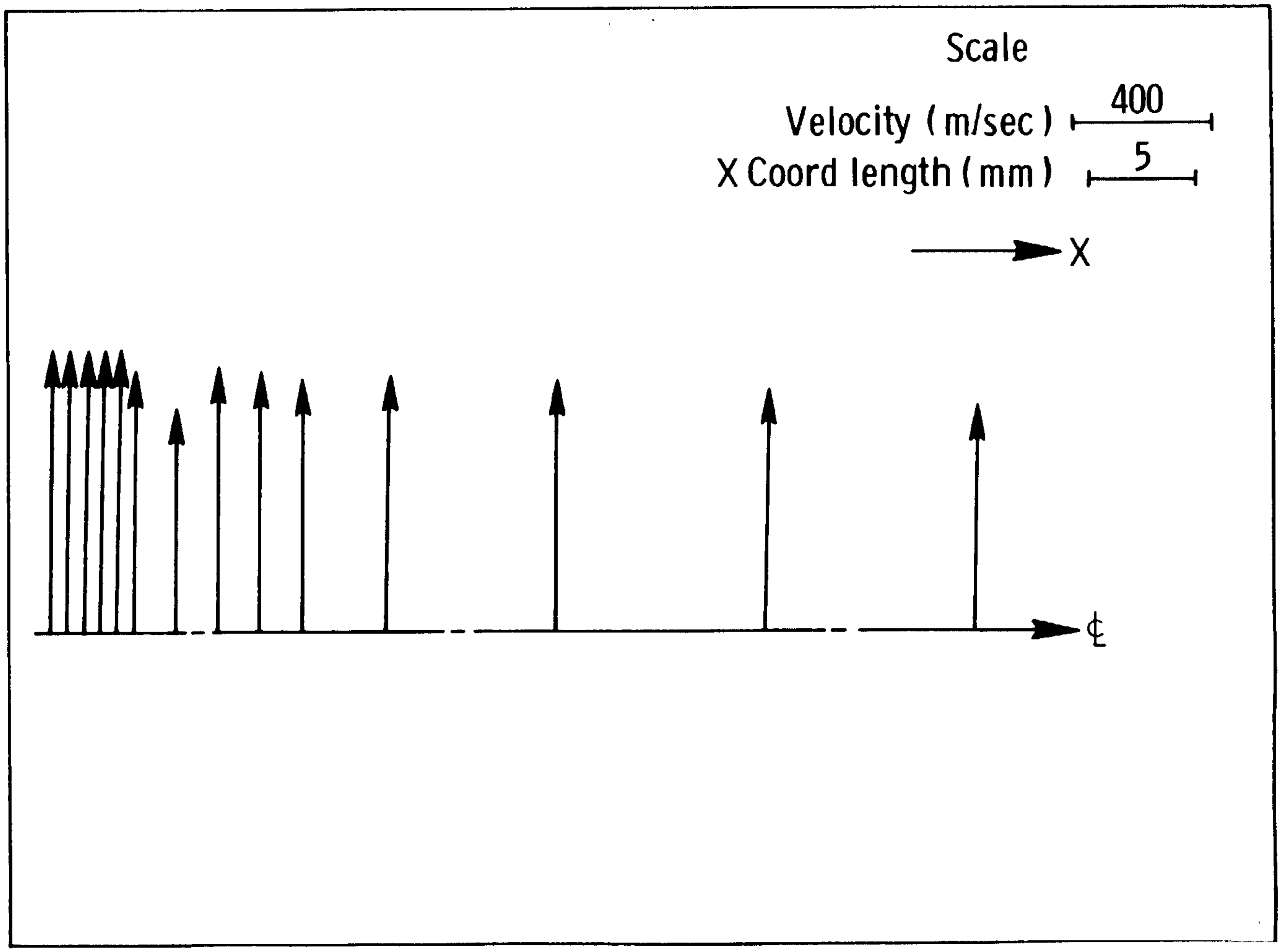

Figure 13. - High velocity interpretation of multimode correlograms of velocity vector measurements along nozzle centerline, Z-position 0.00 mm. Velocity vectors rotated 90° ccw for clarity of presentation. X-coordinate range is 162.60 to 203.20 mm.

NASA

Report Documentation Page

1. Report No.	2. Government Accession No.	3. Recipient's Catalog No.
NASA TM-102725		

4. Title and Subtitle	5. Report Date
Laser Transit Anemometer Measurements of a JANNAF Nozzle Base Velocity Flow Field	August 1990
	6. Performing Organization Code
7. Author(s)	8. Performing Organization Report No.
W. W. Hunter, Jr. C. E Russ, Jr. J. I. Clemmons, Jr.	
	10. Work Unit No.
	505-61-01-06
9. Performing Organization Name and Address	11. Contract or Grant No.
NASA Langley Research Center Hampton, VA 23665-5225	
	13. Type of Report and Period Covered
12. Sponsoring Agency Name and Address	Technical Memorandum
National Aeronautics and Space Administration Washington, DC 20546-0001	14. Sponsoring Agency Code

15. Supplementary Notes

W. W. Hunter, Jr., and C. E Russ, Jr.: Langley Research Center, Hampton, Virginia.
J. I. Clemmons, Jr.: Vigyan Research Associates, Inc., Hampton, Virginia.

16. Abstract

Velocity flow fields of a nozzle jet exhausting into a supersonic flow were surveyed. The measurements were obtained with a laser transit anemometer (LTA) system in the time domain with a correlation instrument. The laser transit anemometer data is transformed into the velocity domain to remove the error that occurs when the data is analyzed in the time domain. The final data is shown in velocity vector plots for positions upstream, downstream, and in the exhaust plane of the jet nozzle.

17. Key Words (Suggested by Author(s))	18. Distribution Statement
Laser Velocimeter Laser Transit Anemometer	Unclassified-Unlimited Subject Category 35

19. Security Classif. (of this report)	20. Security Classif. (of this page)	21. No. of pages	22. Price
Unclassified	Unclassified	26	A03

NASA FORM 1626 OCT 86